

Influence of the synthesis conditions on gallium sulfide thin films prepared by modulated flux deposition

This content has been downloaded from IOPscience. Please scroll down to see the full text.

2009 J. Phys. D: Appl. Phys. 42 085108

(<http://iopscience.iop.org/0022-3727/42/8/085108>)

View [the table of contents for this issue](#), or go to the [journal homepage](#) for more

Download details:

IP Address: 194.29.175.63

This content was downloaded on 30/05/2017 at 15:12

Please note that [terms and conditions apply](#).

You may also be interested in:

[Gallium indium sulfide layers obtained by modulated flux deposition](#)

C Sanz, C Guillén and M T Gutiérrez

[Annealing of indium sulfide thin films prepared at low temperature by modulated flux deposition](#)

C Sanz, C Guillén and J Herrero

[Substrate temperature dependent physical properties of In₂S₃ films](#)

N Revathi, P Prathap, Y P V Subbaiah et al.

[Deposition and characterization of Ga₂Se₃ thin films prepared by a novel CCSVT technique](#)

M Rusu, S Wiesner, S Lindner et al.

[Amorphous to polycrystalline transition in Sb₂S₃ thin films](#)

F Perales, G Lifante, F Agulló-Rueda et al.

[Deposition of ultra thin CuInS₂ absorber layers by ALD for thin film solar cells at low temperature \(down to 150 °C\)](#)

Nathanaelle Schneider, Muriel Bouttemy, Pascal Genevée et al.

[Factors influencing properties of indium tin oxide thin films](#)

R X Wang, C D Beling, S Fung et al.

[Structure and optical properties of thin As₂S₃–In₂S₃ films](#)

R Todorov, D Tsankov, J Pirov et al.

[The use of complex compounds in chemical vapour deposition](#)

Valentin Bessergenev

Influence of the synthesis conditions on gallium sulfide thin films prepared by modulated flux deposition

C Sanz, C Guillén and M T Gutiérrez

Departamento de Energía, CIEMAT, Avda Complutense 22, Madrid 28040, Spain

E-mail: carlos.sanz@ciemat.es

Received 16 December 2008

Published 26 March 2009

Online at stacks.iop.org/JPhysD/42/085108

Abstract

Gallium sulfide thin films were deposited on soda-lime glass substrates by Modulated Flux Deposition (MFD). Using a low deposition rate (1 Å s^{-1}), 100 nm thick layers were prepared at temperatures ranging from 450 to 150 °C with a variable supply of elemental sulfur. EDX analysis showed that these films approached the MX stoichiometry; they corresponded to sulfur-deficient GaS. By raising the availability of sulfur, the bandgap energy (E_g) was increased from 3.2 to 3.6 eV at 350 °C, while it remained constant ($\sim 3.6 \text{ eV}$) at 150 °C; these high E_g values were mainly attributed to quantum size effects. Therefore, high-transmission GaS thin layers can be prepared at only 150 °C by MFD.

(Some figures in this article are in colour only in the electronic version)

1. Introduction

III–VI semiconductor compounds are promising materials for optoelectronic and photovoltaic applications. Among them, gallium sulfides are effective surface passivation layers in III–V semiconductor devices [1, 2]. Besides, gallium sulfide films might replace the CdS buffer layer in CdTe-based solar cells [3] as well as in Cu(In,Ga)(S,Se)₂-based solar cells, in a similar way to In₂S₃ films [4].

In regard to the gallium–sulfur phase diagram, gallium sulfide exhibits two stoichiometries: GaS and Ga₂S₃ [5]. Hexagonal gallium monosulfide (β -GaS), which is the stable MX phase at any temperature, has a layered structure. It consists of four-layered slabs (each one having two close-packaged gallium atom layers and two close-packaged sulfur atom layers arranged according to the stacking sequence S–Ga–Ga–S); there are strongly covalent gallium–sulfur chemical bonds within the slabs, while there are weak interactions (van der Waals forces) between neighbouring slabs [6]. Regarding gallium sesquisulfide (Ga₂S₃), there exist four polytypes, the most stable structure at normal conditions having monoclinic symmetry (α -Ga₂S₃); the remaining phases are hexagonal (α'), defective wurtzite-type (β) and defective blende-type (γ) [7].

Both gallium sulfides are wide-bandgap semiconductors. β -GaS and α -Ga₂S₃ have been assigned bandgap energies (E_g) of 3.05 eV and 3.42 eV at 77 K, respectively [8]. Other authors that deposited Ga–S layers reported a direct bandgap of 3.0 eV for β -GaS [9] and a direct bandgap of 3.31 eV for α -Ga₂S₃ [10].

GaS may show n-type as well as p-type conductivity; the sulfur vacancies act as donors, while the gallium vacancies would act as acceptors [11]. On the other hand, Ga₂S₃ exhibits p-type conductivity [12].

Concerning the synthesis of gallium sulfide layers, they are mostly prepared by single-source metal-organic chemical vapour deposition (MOCVD) methods [13–18]. In these techniques the design of the deposition chamber, the molecular precursor and the substrate temperature strongly affect the stoichiometry and the crystalline structure of the films. For example, amorphous, cubic (metastable) or hexagonal GaS films were deposited by ambient pressure MOCVD between 380 and 420 °C depending on the selected monoprecursor [17], while α -Ga₂S₃ or γ -Ga₂S₃ films were obtained by low pressure MOCVD from a gallium isopropylthiolate when the temperature was changed between 350 and 610 °C [18]. Apart from MOCVD, gallium sulfide films can be obtained by physical vapour deposition (PVD) methods [9, 10, 19–21] but not by chemical bath deposition (CBD), as they become unstable in aqueous solutions [22].

In regard to modulated flux deposition (MFD), indium sulfide and gallium indium sulfide films have already been studied [23], while pure gallium sulfide films had not been investigated yet. Now Ga–S layers have been prepared by MFD for the first time; this paper is focused on their chemical, structural, optical and microstructural properties.

2. Experimental

In our MFD setup the substrate is transported by a carousel-like holder. Then, it follows a cyclical circular path, moving through three different regions inside the vacuum chamber that correspond to the gallium evaporation source, the sulfur evaporation source and an array of halogen lamps that heats the substrate, respectively. By this means, the vapour fluxes from both evaporation sources condense alternately on the heated substrate as elemental quasi-monolayers, so the chemical reaction takes place by surface rather than bulk diffusion processes, and the sulfide can be formed at lower temperatures than usual.

Gallium (99.999%) was evaporated using a Knudsen-type cell, and sulfur (99.999%) was evaporated from a home-designed valved two-zone glass cell. While a constant gallium evaporation temperature was maintained ($T_{\text{Ga}} = 960^\circ\text{C}$), the sulfur evaporation temperature ($220^\circ\text{C} > T_{\text{S}} > 160^\circ\text{C}$) as well as the substrate temperature ($450^\circ\text{C} > T > 150^\circ\text{C}$) were widely varied. In these experiments, Ga–S layers were deposited on soda-lime glass substrates that rotated at 30 rpm, the base pressure being $P_0 \sim 3 \times 10^{-4}$ Pa and the average deposition pressure $P \geq 1 \times 10^{-3}$ Pa. Approximately 100 nm thick layers were obtained at a deposition rate of 1 \AA s^{-1} .

The chemical composition was determined by energy dispersive x-ray analysis (EDX) using a Hitachi S-2500 scanning electron microscope (SEM) with an acceleration voltage of 25 kV. Chemical analyses were also performed by x-ray photoelectron spectroscopy (XPS) with Al $K\alpha 1$ radiation (1486.6 eV) using an argon ion beam sputtering process (15 kV, 25 mA). The structure of the layers was analysed by x-ray diffraction (XRD) using a Phillips X'Pert apparatus with nickel-filtered Cu $K\alpha 1$ radiation. The optical properties were determined by measuring the transmittance and the reflectance at normal incidence from 300 to 1800 nm with a Perkin-Elmer Lambda 9 UV/VIS/NIR spectrophotometer. Surface images were taken with a JEOL JSM 6335 field emission scanning electron microscope (FESEM). The thickness of the films was determined by means of a DEKTAK eight surface profilometer. Their linear absorption coefficient (α) was calculated from equation (1), a relation among the transmittance T , the reflectance R and the film thickness d used in similar investigations [19, 24–26]:

$$e^{-\alpha d} = \frac{\sqrt{((1-R)^4/T^2) + 4R^2} - ((1-R)^2/T)}{2R^2}. \quad (1)$$

Once α was obtained, a direct optical bandgap energy (E_g) was estimated by plotting $(\alpha h\nu)^2$ versus $h\nu$ and making a linear extrapolation in the absorption edge region.

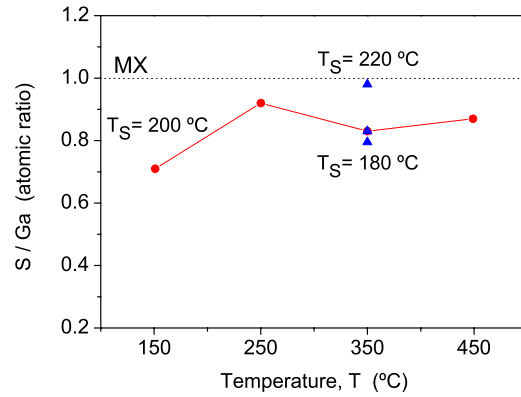


Figure 1. EDX chalcogen/metal atomic ratios as a function of the substrate temperature T (●) at a constant sulfur evaporation temperature ($T_{\text{S}} = 200^\circ\text{C}$) and as a function of the supply of sulfur T_{S} (▲) at a constant substrate temperature ($T = 350^\circ\text{C}$).

Table 1. XPS chemical analyses of two Ga–S thin films, deposited at 350 and 150°C for a maximum delivery of sulfur, as a function of the Ar^+ sputtering time (t).

| T ($^\circ\text{C}$) | t (min) | Ga (at%) | S (at%) | O (at%) | C (at%) | S/Ga |
|-----------------------------|--------------|-------------|------------|------------|------------|------|
| 350 | 0 | 29.0 | 22.0 | 26.4 | 22.7 | 0.76 |
| | 1 | 48.4 | 32.7 | 19.0 | 0 | 0.68 |
| | 3 | 52.8 | 30.5 | 16.7 | 0 | 0.58 |
| 150 | 0 | 26.5 | 21.3 | 33.8 | 18.3 | 0.80 |
| | 1 | 43.5 | 25.7 | 24.6 | 6.2 | 0.59 |
| | 3 | 47.7 | 28.0 | 20.7 | 3.6 | 0.59 |

3. Results and discussion

3.1. Chemical characterization

First, a set of Ga–S thin films was prepared by fixing both gallium and sulfur source temperatures ($T_{\text{Ga}} = 960^\circ\text{C}$ and $T_{\text{S}} = 200^\circ\text{C}$) and reducing the substrate temperature (T) from 450 to 150°C in steps of 50°C . When analysing a selection of these gallium sulfide films by EDX, they showed chalcogen/metal atomic ratios below 1 in the whole range of substrate temperature (figure 1), namely, they approached the MX stoichiometry. Secondly, various Ga–S thin films were deposited with different sulfur supplies at $T = 400^\circ\text{C}$, $T = 350^\circ\text{C}$ ($220^\circ\text{C} > T_{\text{S}} > 180^\circ\text{C}$ in both cases) and $T = 150^\circ\text{C}$ ($200^\circ\text{C} > T_{\text{S}} > 160^\circ\text{C}$). As shown in figure 1 for $T = 350^\circ\text{C}$, when T_{S} was increased up to 220°C (so a higher sulfur vapour pressure was reached), the S/Ga atomic ratio almost reached 1; this stoichiometry (MX) has already been observed in gallium-rich Ga–In–S films prepared by MFD with high enough T_{S} values [23].

Regarding the characterization of the surface region, those two layers prepared with the highest maximum supply of sulfur at 350°C ($T_{\text{S}} = 220^\circ\text{C}$) and 150°C ($T_{\text{S}} = 200^\circ\text{C}$) were analysed by XPS.

These XPS analyses, which were extended up to 3 min of Ar^+ sputtering, are shown in table 1. Before the sputtering process, gallium, sulfur, oxygen and carbon were detected in both samples. After the sputtering process, the carbon

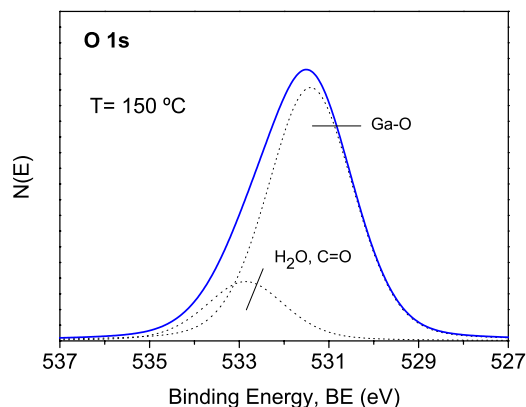


Figure 2. XPS signal corresponding to the O 1s photopeak of a Ga–S thin film prepared at $T = 150\text{ °C}$ with $T_s = 200\text{ °C}$ (before Ar^+ sputtering).

surface contamination was mostly or totally removed, while the oxygen content decreased.

As sulfur is far more volatile than gallium and, unlike gallium, the intensity of its main photopeak did not increase after 1 min of Ar^+ sputtering (despite the removal of the detected surface contamination), it can be assumed that sulfur preferential sputtering took place, namely, S/Ga atomic ratios were underestimated to some extent by XPS.

Regarding the oxygen, the Gaussian–Lorentzian deconvolution of the O 1s photopeak (singlet) provided two signals having the same binding energies in both samples; figure 2 shows those corresponding to the film prepared at 150 °C . In both layers, the minor signal located at 531.5–531.6 eV, which disappeared totally after 3 min of Ar^+ sputtering, was attributable to surface contamination (H_2O , $\text{C}=\text{O}$) adsorbed by air exposure. The major signal located at 535.5–531.6 eV, which remained after the sputtering process, corresponded to oxygen–metal bonds as referenced for gallium oxide (Ga_2O_3) [27].

With respect to the $\text{Ga } 2p^{3/2}$ photopeak, reference data are incomplete, as current bibliography indicates binding energy values of 1116.5–1116.7 eV for metallic gallium [28], 1116.9–1119.6 eV for Ga_2O_3 [13, 27, 28] and 1117.8–1119 eV for Ga_2S_3 [15], but does not mention GaS. Both Ga–S films had a $\text{Ga } 2p^{3/2}$ photopeak located at 1118.5–1118.6 eV (that corresponded to our gallium sulfide), as figure 3 shows for the layer deposited at 150 °C . When deconvoluting it, a single signal (1118.5 eV) was observed at 350 °C , while two chemical states appeared at 150 °C , indicating that gallium sulfide and/or oxide (1118.4 eV) existed as well as a small amount of gallium metal (1117.0 eV); the extremely weak contribution located at 1120.5 eV is a deconvolution artefact that does not correspond to any chemical compound.

The Auger lines showed that the surface of the GaS film prepared at a higher temperature (350 °C) had a more complex mixture of chemical states (figure 4). According to the bibliography, the $\text{Ga } L_3M_{45}M_{45}$ Auger line (expressed as kinetic energy) is located at 1061.6–1063.2 eV for Ga_2O_3 [13], 1064.6 eV for Ga_2S_3 [15] and 1066.2–1068.2 eV for metallic gallium [28], while GaS has not been referenced yet. Due to its intrinsic nature, the $\text{Ga } L_3M_{45}M_{45}$ Auger emission is an asymmetric signal that consists of a main peak (maximum

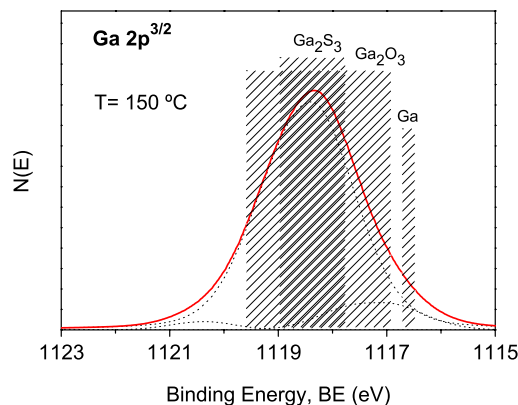


Figure 3. XPS signal corresponding to the $\text{Ga } 2p^{3/2}$ photopeak of a Ga–S thin film prepared at $T = 150\text{ °C}$ with $T_s = 200\text{ °C}$ (before Ar^+ sputtering).

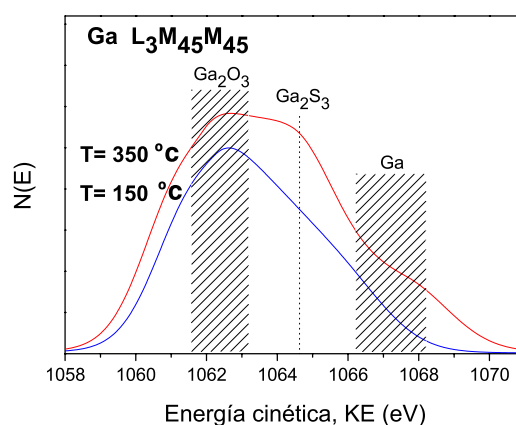


Figure 4. XPS signals corresponding to the $\text{Ga } L_3M_{45}M_{45}$ Auger emissions of two Ga–S thin films prepared at $T = 350\text{ °C}$ and $T = 150\text{ °C}$ for a maximum supply of sulfur (after 1 min of Ar^+ sputtering).

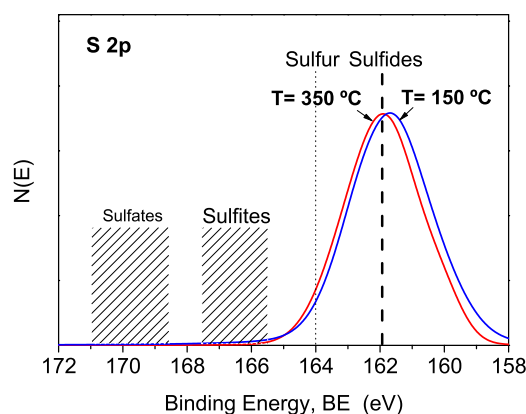


Figure 5. XPS signals corresponding to the S 2p photopeaks of two Ga–S thin films prepared at $T = 350\text{ °C}$ and $T = 150\text{ °C}$ for a maximum supply of sulfur (before Ar^+ sputtering).

intensity) with a shoulder (lower intensity) in the highest-energy side. As shown in figure 4, although the two Auger spectra had different shapes, the maximum was located around 1062 eV in both cases.

In any case, figure 5 shows that the S 2p doublet had a binding energy of 162 eV, which is a typical value for

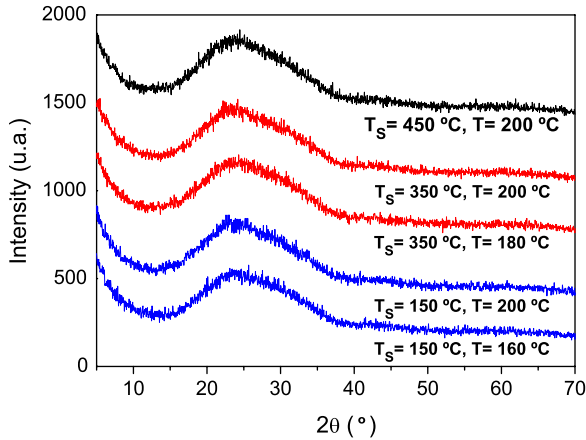


Figure 6. X-ray diffractograms of gallium sulfide thin films prepared at different sulfur temperatures (T_S) and substrate temperatures (T).

sulfides [32]. It confirmed the reaction between gallium and sulfur to form the sulfide at both substrate temperatures (350 and 150 °C); other possible sulfur chemical states (sulfite, sulfate, elemental sulfur) were discarded.

3.2. Structural properties

Even though the low deposition rate (1 Å s^{-1}) favoured the reaction between both evaporated elements (in fact, gallium sulfide was formed even at a substrate temperature as low as 150 °C, as confirmed by XPS analysis), the x-ray diffractograms indicated that all the Ga–S films were amorphous. As shown in figure 6, polycrystalline films were not formed either by the increase in the substrate temperature up to 450 °C or by the increase in the sulfur delivery.

In a previous work [23], gallium-rich Ga–In–S films (atomic ratio Ga/In ~ 9) were prepared at 350 °C at deposition rates of $1\text{--}2 \text{ Å s}^{-1}$ by MFD. Then, a high enough supply of sulfur provided highly transparent amorphous MX layers (in a similar way to the results obtained in the present work), while more limited supplies of sulfur provided lower-transmission metal-rich layers, which contained β -GaS as confirmed by their diffractograms.

3.3. Optical properties

The optical properties of the series of 100 nm thick Ga–S films deposited at 350 and 150 °C by providing different fluxes of sulfur were compared. Figure 7 shows the transmittance curves of the layers prepared at 350 °C.

In this case, it was clear that the gradual increase in the availability of sulfur provided more transparent layers. As a consequence, the optical absorption edge became more abrupt and shifted towards higher energies (figure 7), and the bandgap energy (E_g) increased from 3.2 to 3.6 eV (figure 8(a)). Identical optical behaviour was observed in the set of 100 nm thick Ga–S films prepared at 400 °C with different sulfur supplies (not shown here).

Nevertheless, the optical properties of the Ga–S films prepared at 150 °C did not show significant changes with regard

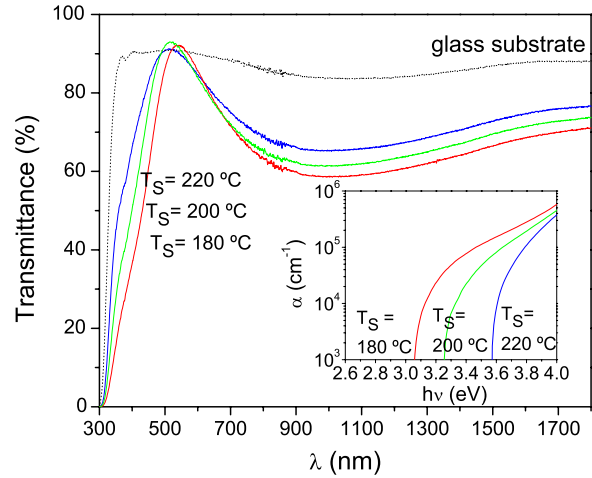


Figure 7. Transmittance and absorption spectra of gallium sulfide thin films ($d \sim 100 \text{ nm}$) prepared at $T = 350 \text{ °C}$ for different sulfur evaporation temperatures (T_S).

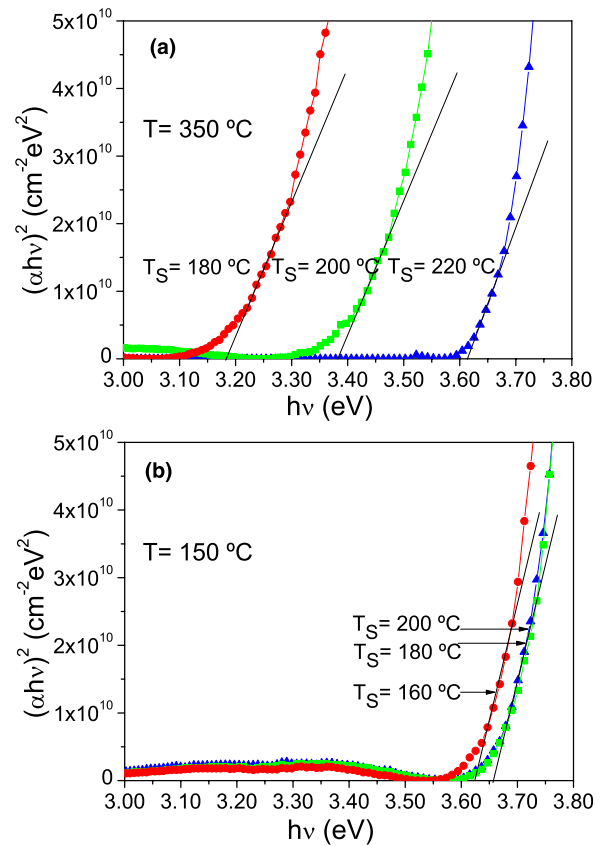


Figure 8. Bandgap energy (E_g) estimated by linear extrapolation for gallium sulfide thin films ($d \sim 100 \text{ nm}$) prepared at (a) $T = 350 \text{ °C}$ and (b) $T = 150 \text{ °C}$ for different sulfur evaporation temperatures (T_S).

to the variation of the deposition parameter T_S . Indeed, they had similar transmittance curves and their bandgap energies were located around 3.6 eV (figure 8(b)). It equals the maximum value observed at 350 °C, when the highest sulfur flux was delivered. Therefore, the E_g values of these MFD-grown Ga–S films were larger than those corresponding to amorphous GaS layers directly evaporated and post-annealed

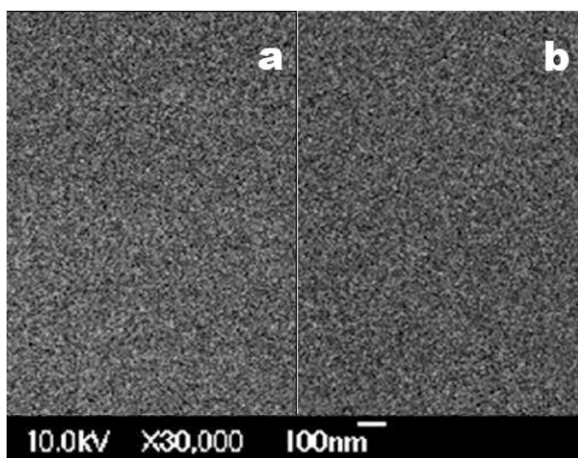


Figure 9. FESEM surface images (30 000×) of Ga-S thin films (thickness = 100 nm) prepared at (a) 350 °C and (b) 150 °C with a maximum supply of sulfur.

($E_g = 2.7$ eV) [19] or to β -GaS films prepared by reactive sputtering ($E_g = 3.0$ eV) [9], as well as those of MFD-grown gallium-rich Ga-In-S layers [23], whose absorption edge reached 3.2 eV.

The bibliography states that if the average crystallite size (D) of a semiconductor material is small enough, its bandgap energy (E_g) may increase due to quantum size effects [29–31]. Taking this into account, it can be understood that our x-ray amorphous films approaching the GaS composition exhibited E_g values larger than the reported value for gallium monosulfide. In regard to the behaviour observed at high temperatures (400, 350 °C), it could be inferred that the adsorption/incorporation of volatile sulfur at high temperatures was less favourable, so a large supply of sulfur was required to reduce the optical absorption by the reduction of the amount of sulfur vacancies.

Compared with MFD-grown gallium sulfide films with a small content of indium, which had an MX stoichiometry, an amorphous structure and a maximum E_g of 3.2 eV when increasing T_S [23], pure gallium sulfide films provide even larger E_g values.

3.4. Microstructure

Finally, the surface morphology of the largest-bandgap Ga-S films obtained at 350 and 150 °C was analysed by FESEM. MFD has already provided In-S polycrystalline thin layers with small rounded-grain microstructures (average diameter around 100 nm at $T = 310$ °C) [32]. Now, amorphous Ga-S thin layers had very small rounded-grain microstructures (figure 9). Their average diameters were estimated around 15 nm at 350 °C and 12 nm at 150 °C, so there was not a significant effect of the substrate temperature on the microstructure of these Ga-S layers.

4. Conclusions

100 nm thick pure gallium sulfide films were deposited using elemental evaporation sources at a substrate temperature

ranging from 450 to 150 °C by modulated flux deposition (MFD). These films having a stoichiometry near to gallium monosulfide (GaS) and being x-ray-amorphous, their optical properties were only significantly influenced by the availability of sulfur (namely, the experimental parameter T_S) at a high temperature. Hence, when they were prepared at 350 °C, the bandgap energy (E_g) increased with the sulfur supply up to a value as large as 3.6 eV. It was also possible to prepare GaS thin layers with $E_g = 3.6$ eV by MFD at a substrate temperature of 150 °C, which is a very low value for a PVD-type deposition process. In conclusion, the layer deposition technique, named MFD, is capable of providing very high-transmission gallium sulfide layers at quite low substrate temperatures.

Acknowledgments

This work has been supported by the FOTOFLEX-CM Project (S-0505/ENE-O123) of IV PRICIT by Comunidad de Madrid, ‘Células fotovoltaicas ligeras y flexibles’ Project by Fundación Ramón Areces and CONSOLIDER GENESIS FV Project (CSD2006-04)

References

- [1] Cao X A, Hu H T, Ding X M, Yuan Z L, Dong Y, Chen X Y, Lai B and Hou X Y 1998 *J. Vac. Sci. Technol. B* **16** 2656
- [2] Wang X, Chen X Y, Hou X Y, Cao X A, Ding X M, Chen L Y and Zhao G Q 1997 *J. Cryst. Growth* **173** 51
- [3] Cuculescu E, Evtodiev I, Caraman M and Rusu M 2006 *J. Optoelectron. Adv. Mater.* **8** 1077
- [4] Hariskos D, Spiering S and Powalla M 2005 *Thin Solid Films* **480–481** 99
- [5] Lieth R M A, Heijligers H J M and v.d. Heidjen C W M 1966 *J. Electrochem. Soc.* **8** 798
- [6] Lieth R M A (ed) 1977 *Preparation and Crystal Growth of Materials with Layered Structures* (Dordrecht: Reidel)
- [7] Pardo M P, Guitard M, Chilouet A and Tomas A 1993 *J. Solid State Chem.* **102** 423
- [8] Madelung O and Poerschke R (eds) 1992 *Semiconductor: Other than Group IV Elements and III-V Compounds* (Berlin: Springer)
- [9] Ohyama M, Ito H and Takeuchi M 2005 *Japan. J. Appl. Phys.* **44** 4780
- [10] Kim W T, Kin H S, Kim Y G and Hahn S R 1987 *J. Mater. Sci. Lett.* **6** 479
- [11] Lieth R M A and Van der Maesen F 1972 *Phys. Status. Solidi. A* **10** 73
- [12] Belal A E, Elshaikh H A and Ashraf I M 1994 *Crys. Res. Technol.* **7** K92
- [13] Pernot P J and Barron A R 1995 *Chem. Vapor Depos.* **1** 75
- [14] Keys A, Bott S G and Barron A R 1999 *Chem. Mater.* **11** 3578
- [15] Lazell M R, O’Brien P, Otway D J and Park J H 1999 *Chem. Mater.* **11** 3430
- [16] Duesler E N, Hampdensmith M J and Shang G H 1996 *Chem. Commun.* **37** 1733
- [17] MacInnes A N, Power M B, Hepp A F and Barron A R 1993 *Chem. Mater.* **5** 1344
- [18] Suh S and Hoffman D M 2000 *Chem. Mater.* **12** 2794
- [19] Micocci G, Rella R and Tepore A 1989 *Thin Solid Films* **172** 179
- [20] Morii K, Ikeda H and Nakayama Y 1993 *Mater. Lett.* **17** 274

- [21] Yamada H, Ueno K and Koma A 1996 *Japan. J. Appl. Phys.* **35** L568
- [22] Boyle D S, Govender K, Hazelton R L and O'Brien P 2003 *203rd Meeting of the Electrochemical Society (Paris, France, 2003)*
- [23] Sanz C, Guillén C and Gutiérrez M T 2007 *Phys. Stat. Sol. A* **204** 3367
- [24] Timoumi A, Bouzouita H, Kanzari M and Rezig B 2005 *Thin Solid Films* **480-481** 124
- [25] Calixto-Rodríguez M, Tiburcio-Silver A, Ortiz A and Sánchez-Juárez A 2005 *Thin Solid Films* **480-481** 133
- [26] Asenjo B, Chaparro A M, Gutiérrez M T, Herrero J and Maffiotte C 2004 *Electrochim. Acta* **49** 737
- [27] Kim D H, Yoo S H, Chung T M, An K S, Yoo H S and Kim Y 2002 *Bull. Korean Chem. Soc.* **23** 225
- [28] Passlack M, Schubert E F, Hobson W S, Hong M, Moriya N and Chu S N G 1995 *J. Appl. Phys.* **77** 686
- [29] Yoshida T, Yamaguchi K, Toyoda H, Akao K, Sugiura T, Minoura H and Nosaka Y 1997 *Electrochem. Soc. Proc.* **97** 37
- [30] Yasaki Y, Sonoyama N and Sakata T 1999 *J. Electroanal. Chem.* **469** 116
- [31] Kosaraju S, Marino J A, Harvey J A and Wolden C A 2006 *Sol. Energy Mater. Sol. Cells* **90** 1121
- [32] Sanz C, Guillén C and Gutiérrez M T 2006 *Thin Solid Films* **511-512** 121